

Dynamics analysis of Wien-bridge hyperchaotic memristive circuit system

Xiaolin Ye · Jun Mou  · Chunfeng Luo · Zhisen Wang

Received: 8 September 2017 / Accepted: 21 January 2018 / Published online: 8 March 2018
© Springer Science+Business Media B.V., part of Springer Nature 2018

Abstract In this paper, a hyperchaotic memristive circuit based on Wien-bridge chaotic circuit was designed. The mathematical model of the new circuit is established by using the method of normalized parameter. The equilibrium point and the stability point of the system are calculated. Meanwhile, the stable interval of corresponding parameter is determined. Using the conventional dynamic analysis method, the dynamical characteristics of the system are analyzed. During the analysis, some special phenomenon such as coexisting attractor is observed. Finally, the circuit simulation of system is designed and the practical circuit is realized. The results of theoretical analysis and numerical simulation show that the Wien-bridge hyperchaotic memristive circuit has very rich and complicated dynamical characteristics. It provides a theoretical guidance and a data support for the practical application of memristive chaotic system.

Keywords Hyperchaotic memristive circuit · Lyapunov exponents · Coexisting attractor · Circuit simulation

1 Introduction

The Academia have never stopped studying and exploring for the chaotic systems. The most classic system is the 3D continuous autonomous chaotic system [1–3]. However, the research for chaotic memristive system has gradually become a hot academic research in recent years. The good nonlinear characteristics of memristor can perfectly combine with the chaotic system [4–7]. All the signs indicate that memristor would be the most potential electronic element.

Memristor is a nonlinear resistance with memory function [8,9]. It can change its resistance value by controlling the current variation, and this variation can continue to maintain even if the power goes off. So, these advantages above make memristor become a natural nonvolatile memory [10,11]. In particular, the good memory characteristic of memristor will produce a profound influence on the fields of computer science [12,13], bioengineering [14,15], neural network [16,17], electronic engineering [18,19] and control engineering [20–24]. Meanwhile, the existence of memristor also makes the number of basic circuit element increased to four. However, memristor is a nano component [25–30], so it requires much higher technology content to physically implement. It indicated that memristor will not be used in commercial and civilian in a short time.

Generally, memristor include flux-controlled memristor [31] and charge-controlled memristor [32]. The organic combination of memristor and other compo-

X. Ye · J. Mou (✉) · C. Luo · Z. Wang
School of Information Science and Engineering, Dalian
Polytechnic University, Dalian 116034, China
e-mail: moujun@csu.edu.cn

nents can compose a chaotic memristive circuit. In particular, the researches on its complicated dynamical characteristics have become a mainstream in the direction of chaotic memristive circuit system [8,33–35]. Meanwhile, in the field of chaotic circuit, the most popular research is based on the circuit model of Chua [36]. But the researches based on these hot circuit model will be saturated one day. Thus, it is very necessary to develop a new chaotic memristive circuit model.

The Wien-bridge circuit is a RC oscillating circuit, and it has the characteristics of oscillating stabilization and good waveform. Adding two anti-parallel diodes and a LC parallel circuit to the classical 2D Wien-bridge chaotic circuit [37], which can constitute a 4D Wien-bridge chaotic circuit. Then, we use a flux-controlled memristor [38,39] to replace a resistance of the 4D Wien-bridge chaotic circuit. Finally, a new 5D Wien-bridge hyperchaotic memristive circuit model is established.

In this article, we focus on the new Wien-bridge hyperchaotic circuit. It is organized as follows. In Sect. 2, the model of memristive circuit is presented, and the new mathematical model of normalized parameter was established. In Sect. 3, the stability of the equilibrium set was analyzed. In Sect. 4, the dynamical characteristics of system were analyzed by Lyapunov exponents spectrum, bifurcation diagrams, spectral entropy (SE) and C_0 complexity. The phenomenon of coexisting attractor was observed, and the mode of coexisting bifurcation was found. Finally, the practical circuit of Wien-bridge hyperchaotic memristive circuit was realized. It make theoretical analysis and practical circuit unity. This article opens up a new model of hyperchaotic memristive circuit and a creative idea of mathematical modeling, and it also provides a theoretical guidance for the practical application of chaotic memristive circuit.

2 Wien-bridge hyperchaotic memristive circuit

2.1 Model of circuit

We use a flux-controlled memristor to replace a resistance R_1 of 4D Wien-bridge chaotic circuit. Then, a new 5D Wien-bridge hyperchaotic circuit is built. Figure 1 shows that the circuit consists of three capacitors C_1, C_2, C_3 , an operational amplifier, two nonlin-

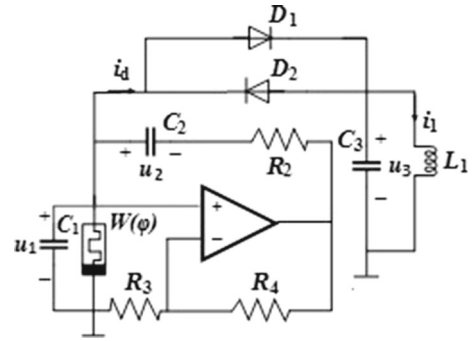


Fig. 1 5D Wien-bridge memristive hyperchaotic circuit

ear diodes D_1, D_2 and three resistances and a flux-controlled memristor. U_1, U_2, U_3 are the corresponding voltages of three capacitors.

2.2 Mathematical model

The new Wien-bridge memristive circuit is a 5D circuit system. There is a large gap in the numerical value of components. So, we have to do the normalized parameter processing for the initial circuit equations, and then the new mathematical model are established. According to the Kirchhoff’s current and voltage laws and voltage–current characteristics of all components, we obtain the differential equation:

$$\begin{cases} C_1 \frac{du_1}{dt} = \frac{R_4}{R_2 R_3} u_1 - w(\phi) u_1 - \frac{u_2}{R_2} - i_d \\ C_2 \frac{du_2}{dt} = \frac{R_4}{R_2 R_3} u_1 - \frac{u_2}{R_2} \\ C_3 \frac{du_3}{dt} = i_d - i_1 \\ L_1 \frac{di_1}{dt} = u_3 \\ \frac{d\phi}{dt} = u_1 \end{cases}, \quad (1)$$

where the voltage–current characteristics of two anti-parallel diodes is:

$$i_d = g_d [u_1 - u_3 + 0.5(|u_1 - u_3 - U_{th}| - |u_1 - u_3 + U_{th}|)], \quad (2)$$

in which U_{th} is the threshold voltage of diode, and g_d is the forward turn-on conductance.

$$\begin{cases} q(\phi_1) = a\phi_1 + b_1\phi_1^3 \\ W(\phi_1) = a + 3b_1\phi_1^2 \end{cases}, \quad (3)$$

Fig. 2 Hyperchaotic attractor of the system. **a** $x - z$ plane. **b** $y - z$ plane

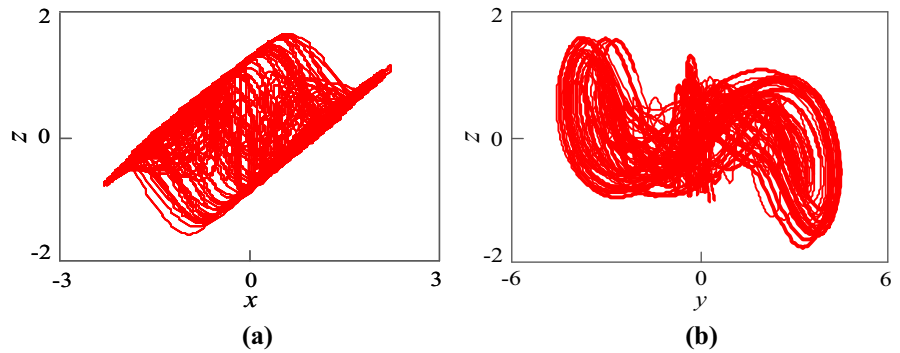
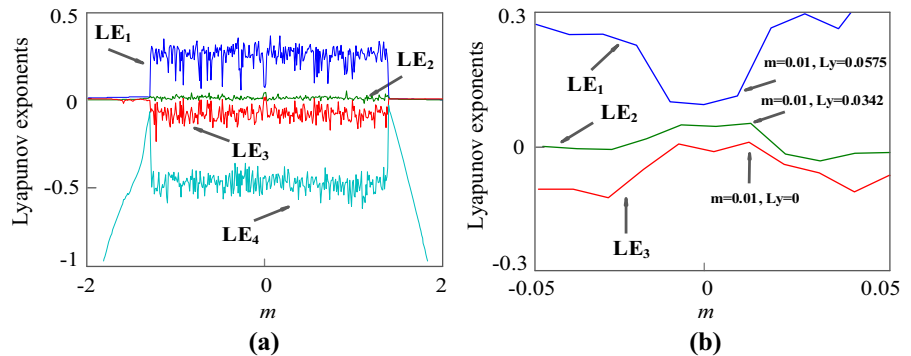


Fig. 3 Lyapunov exponents spectrum with varying m . **a** Range of m is $[-2, 2]$. **b** Range of m is $[-0.05, 0.05]$



where, $W(\varphi)$ is the memductance, a and b_1 are the real constant.

Let $u_1 = U_{th}x, u_2 = U_{th}y, u_3 = U_{th}z, i_1 = U_{th}w/(R_2R_3)^{1/2}, \varphi = U_{th}C_1(R_2R_3)^{1/2}v, i_d = U_{th}H(R_2R_3)^{1/2}gd, t = C_1(R_2R_3)^{1/2}\tau, c = (R_4/R_2)^{1/2}, d = (R_4/R_3)^{1/2}, e = (R_2R_3)^{1/2}, g = (R_2R_3)^{1/2}gd, k = C_1R_2R_3/L_1, C_1 = C_2 = C_3, b = U_{th}^2C_1^2R_2R_3b_1, w(v) = a + 3bv^2$. It's means:

$$H = x - z + 0.5(|x - z - 1| - |x - z + 1|). \tag{4}$$

By employing the normalized operation Eq. (1) becomes to

$$\begin{cases} \dot{x} = [cd - e(a + 3bv^2)]x - yc/d - gH \\ \dot{y} = cdx - yc/d \\ \dot{z} = gH - w \\ \dot{w} = kz \\ \dot{v} = x \end{cases} \tag{5}$$

Obviously, the new circuit system is a 5D system, and it can be described by Eq. (5).

2.3 Hyperchaotic attractor

Setting $a = 0.03, b = 0.02, c = 1.2, d = 2.83, e = 21.21, g = 21.21, k = 21.5$, the initial value of Eq. (5) is $(1, 1, 1, 1, 0.01)$, and the time step is $t = 0.01s$. We can get a hyperchaotic attractor as shown in Fig. 2. In this case, the Lyapunov exponents values are $LE_1 = 0.0575, LE_2 = 0.0342, LE_3 = 0, LE_4 = -0.5051, LE_5 = -27.8043$, and the Lyapunov dimension $d_L = 3.1815$. Obviously, there are two positive values of Lyapunov exponents, so the new circuit is a hyperchaotic system.

3 Characteristic analysis of system

3.1 Symmetry characteristic

The system (5) can remain unchanged after the transformation of $(x, y, z, w, v) \rightarrow (-x, -y, -z, -w, -v)$. So, the system is symmetric about the origin.

3.2 Dissipation characteristic

If the system (5) is a hyperchaotic system, it must meets the condition:

Table 1 Dynamical behaviors with different m

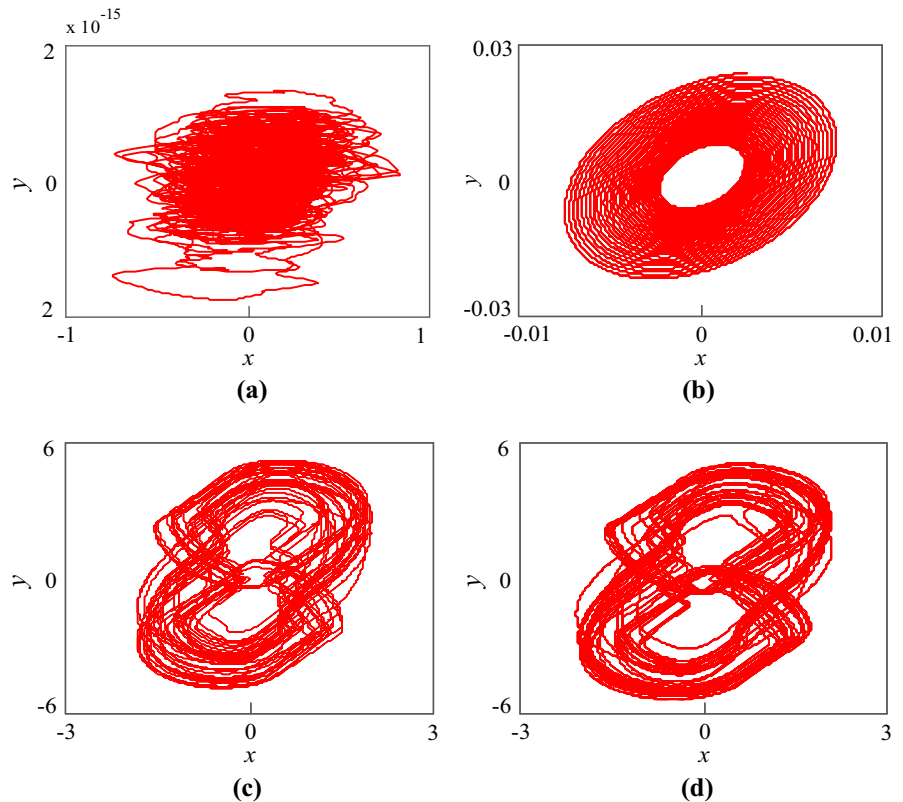
m	Dynamical behaviors
- 4 to - 1.284	Unstable sink
- 1.283	Stable sink
- 1.282 ~ - 0.009	Chaotic attractor
- 0.01 to 0.01	Hyperchaotic attractor
0.011-1.3962	Chaotic attractor
1.3963	Stable sink
1.3964	Chaotic attractor
1.3965-1.3967	Stable sink
1.3968-4	Unstable sink

$$\nabla V = \frac{\partial \dot{x}}{\partial x} + \frac{\partial \dot{y}}{\partial y} + \frac{\partial \dot{z}}{\partial z} + \frac{\partial \dot{w}}{\partial w} + \frac{\partial \dot{v}}{\partial v} < 0 \quad (6)$$

Thus, we can obtain that the condition of system (5) is a hyperchaotic system:

$$cd - 2g \left(\frac{\partial H}{\partial x} - \frac{\partial H}{\partial z} \right) - ew(v) < 0. \quad (7)$$

Fig. 4 Phase portraits with different initial states m . **a** Unstable sink ($m = -2$). **b** Stable sink ($m = -1.283$). **c** Chaotic attractor ($m = -1$). **d** Hyperchaotic attractor ($m = 0.01$)



3.3 Equilibrium points set and analysis of stability

Let $\dot{x} = \dot{y} = \dot{z} = \dot{w} = x = 0$, we get the equilibrium point set $E = [(x, y, z, w, v)|x = y = z = w = 0, v = m]$. So, any point set located on v plane are all equilibrium points, where m is a real constant. Select normalized parameters $a = 0.03, b = 0.02, c = 1.2, d = 2.83, e = 21.21, g = 21.21, k = 21.5$. In which d and m are variable parameters, the Jacobi-matrix in equilibrium points of system. (5) is:

$$J = \begin{bmatrix} 1.2d - 21.21(0.03 + 0.06m^2) & -1.2/d & 0 & 0 & 0 \\ 1.2d & -1.2/d & 0 & 0 & 0 \\ 0 & 0 & 0 & -1 & 0 \\ 0 & 0 & 21.5 & 0 & 0 \\ 1 & 0 & 0 & 0 & 0 \end{bmatrix}. \quad (8)$$

The characteristic root equations of equilibrium point set are :

$$\lambda(\lambda^4 + a_1\lambda^3 + a_2\lambda^2 + a_3\lambda + a_4) = 0, \quad (9)$$

Table 2 Dynamical behaviors with different d

d	Dynamical behaviors
2–2.7	Period-1 cycle
2.71–2.75	Chaotic attractor
2.76	Period-1 windows
2.77	Chaotic attractor
2.78–2.81	Period-1 windows
2.82	Chaotic attractor
2.83–2.84	Hyperchaotic attractor
2.85–2.88	Chaotic attractor
2.89–2.95	Period-3 windows
2.96–3.05	Chaotic attractor
3.06	Hyperchaotic attractor
3.07–4.64	Chaotic attractor
4.65–5	Period-1 cycle

where,

$$a_1 = 1.2726m^2 + 1.2/d + 0.6363 - 1.2d$$

$$a_2 = 1.52712m^2/d + 0.76356/d + 21.5$$

$$a_3 = 27.3609m^2 + 25.8/d + 13.68045 - 25.8d$$

$$a_4 = 32.83308m^2/d + 16.41654/d \tag{10}$$

According to the stability condition of Routh–Hurwitz, the necessary and sufficient condition of all roots have negative real parts are:

$$H_k = \begin{bmatrix} a_1 & a_3 & 0 & 0 \\ 1 & a_2 & a_4 & 0 \\ 0 & a_1 & a_3 & 0 \\ 0 & 1 & a_2 & a_4 \end{bmatrix} > 0, \tag{11}$$

in which, $k = 1, 2, 3, 4$.

$$H_1 = a_1 > 0$$

$$H_2 = a_1a_2 - a_3 > 0$$

$$H_3 = a_1(a_2a_3 - a_1a_4) - a_3^2 > 0$$

$$H_4 = a_4H_3 > 0 \tag{12}$$

Select circuit parameters $d = 2.83$, we can get the stability range of m is :

$$|m| \geq 1.3548. \tag{13}$$

Fig. 5 Dynamical behaviors with different d . **a** Lyapunov exponents. **b** Bifurcation diagram. **c** SE complexity. **d** C_0 complexity

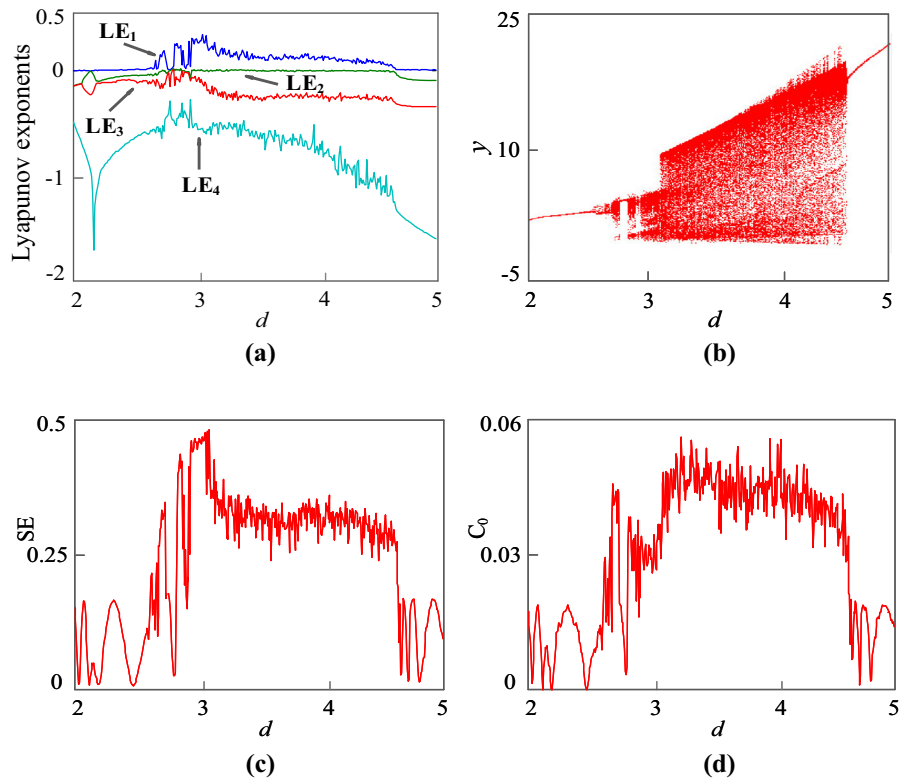
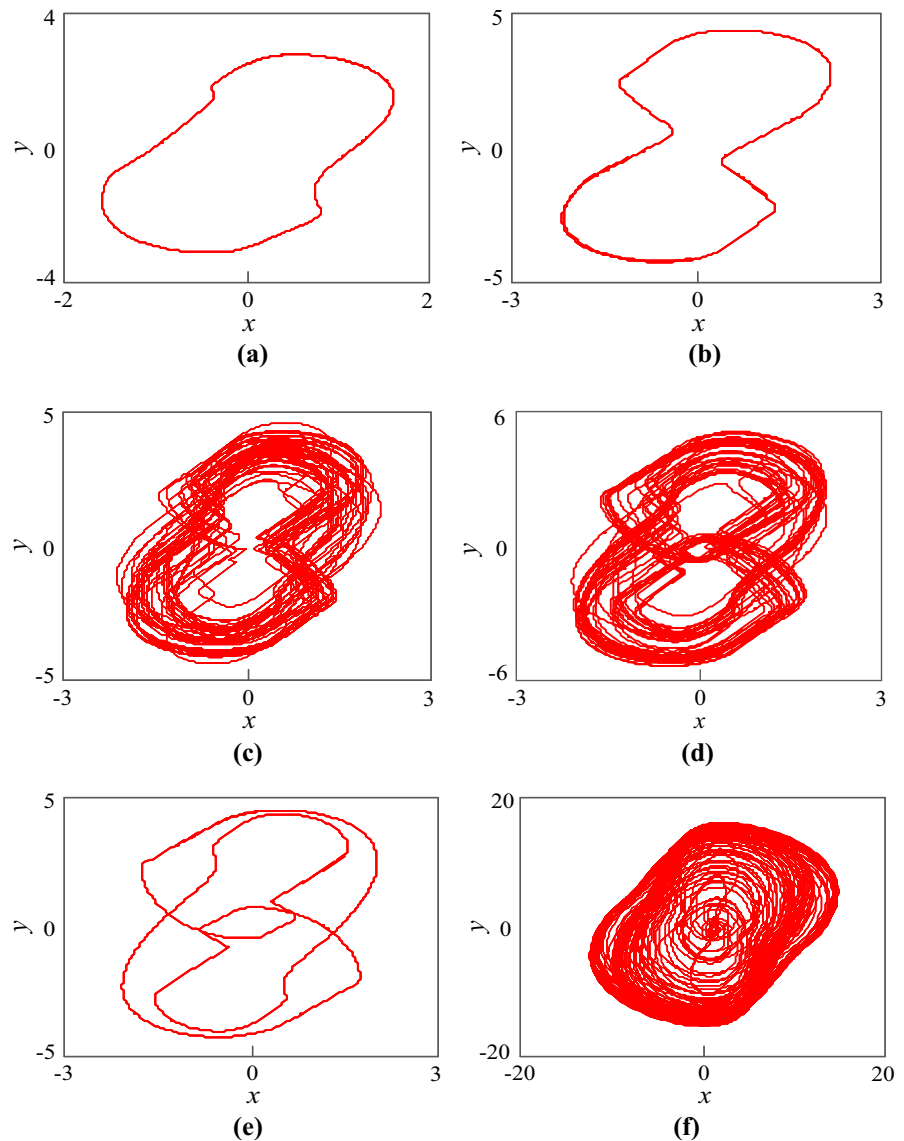


Fig. 6 Phase portraits with different d . **a** Type I period-1 ($d = 2.5$). **b** Type II period-1 ($d = 2.8$). **c** Chaotic attractor ($d = 2.82$). **d** Hyperchaotic attractor ($d = 2.83$). **e** Period-3 windows ($d = 2.9$). **f** Type II chaotic attractor ($d = 4$)



4 Dynamic analysis of hyperchaotic memristive system

4.1 Dynamic analysis with different memristive initial states

The time evolution of system is unpredictable under the different initial conditions, but its track always limited to a certain area. That is to say, the range of chaos is bounded. In order to further studying the nonlinear dynamic characteristics of system, we select the Lyapunov exponents spectrum as a research object.

Keeping other parameters the same as mentioned above, and select the initial value of system is $(1, 1, 1, v(0))$, where $v(0)$ is variable parameter m . Setting the simulation step size is $h = 0.01$, time step is $t = 0.01$ s. The Lyapunov exponents spectrum changing with different initial value m as shown in Fig. 3. In order to better observing and studying, the minimum Lyapunov exponent is ignored. There are two positive Lyapunov exponents can be observed, so the system is a hyperchaotic system. In particular, we select the range of m $[-0.05, 0.05]$ as a study range. As shown in Fig. 3b, we can clearly observe the whole process that the system goes into the hyperchaotic state

Fig. 7 Coexisting attractors with different initial states. **a** Coexisting period-1 ($d = 1.7$). **b** Coexisting chaotic attractor ($d = 1.79$). **c** Type II coexisting period-1 ($d = 2.6$). **d** Type II coexisting hyperchaotic attractor ($d = 2.83$)

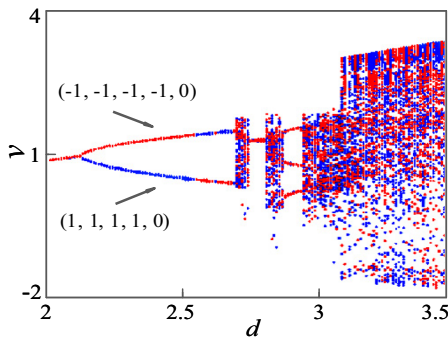
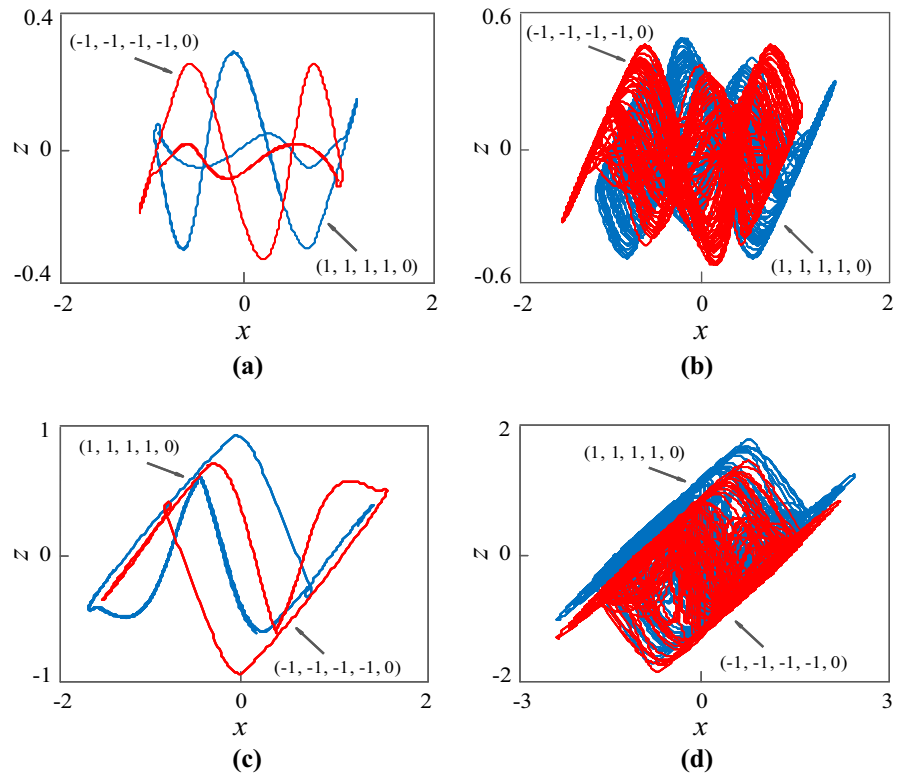


Fig. 8 Coexisting bifurcation diagram

from the chaotic state. The detailed dynamical behaviors of system with different parameter m are summarized in Table 1. However, there are a few differences between numerical simulation and theoretical analysis. It is mainly because the equilibrium points set has a zero characteristic root in addition to the four nonzero characteristic roots.

To further present its dynamic characteristics, $x - y$ phase portraits with different initial states m are presented in Fig. 4. With the increase in m , the system transform from unstable sink to hyperchaotic attractor.

4.2 Dynamical behaviors with different circuit parameter

Keeping other parameters the same as mentioned above and select d is the variable parameter, the initial value of system is $(1, 1, 1, 1, 0.01)$. The dynamical characteristic of system is analyzed by using SE algorithm and C_0 algorithm. It can reflect the complexity of continuous chaotic systems accurately and effectually. With parameter d increasing, the system presents a variety of dynamic characteristics. The range of system into the limit cycle orbit is $[2, 2.7]$. When the system is in the periodic state, the complexity values of corresponding system are very small too. When the range is $[2.71, 2.89]$, the system changes states between chaotic state and hyperchaotic state. In this case, the corresponding complexity value is much larger. If the system (5) is used in the field of secret communication, it is best to choose the parameters within this interval as a secret key. We can see a larger periodic window when the range is $[2.76, 2.82]$, and the corresponding complexity values also sudden decline. When the range is $(3.06, 4.64]$, the chaotic state of system is disappearing, and the corresponding complexity value is much

Fig. 9 Wien-bridge hyperchaotic memristive circuit

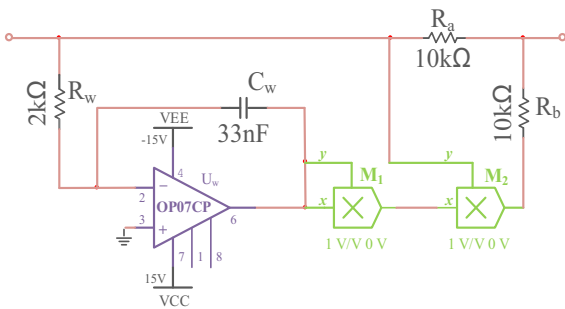
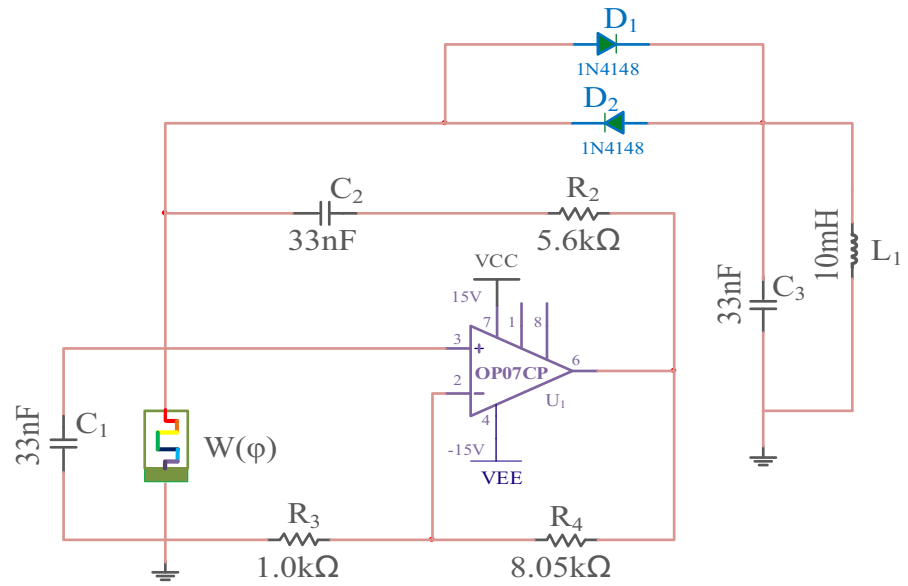


Fig. 10 Equivalent circuit of memristor

smaller, even to 0. The detailed state interval varying with parameter d is shown in Table 2. The varying tendency of numerical simulation reflected in Fig. 5 is basically the same.

In order to more clearly show the complex characteristics of system, $x - y$ phase portraits with different circuit parameter d are presented in Fig. 6. With varying d , the system display different topological structures.

4.3 Coexisting attractor

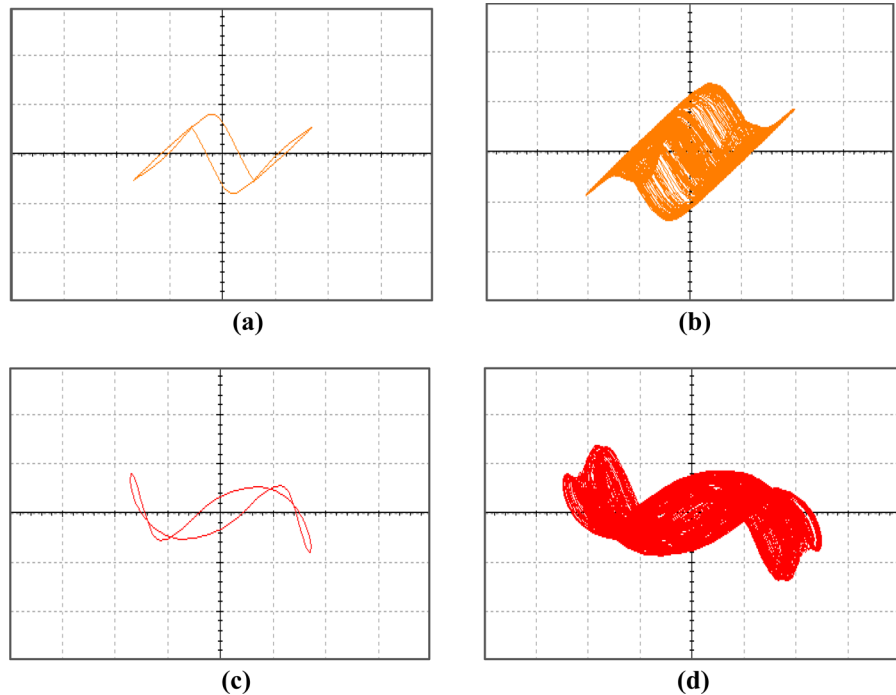
Let parameters $a = 0.03$, $b = 0.02$, $c = 1.2$, $d = 2.83$, $e = 21.21$, $g = 21.21$, $k = 21.5$, and d is the variable parameter. The blue track represents the orbit starts from the initial state $(1, 1, 1, 1, 0)$, while

the red track starts from the initial state $(-1, -1, -1, -1, 0)$. When $d = 1.7$, the system is in the coexisting limit cycles with period-4. With the parameter d increases, the system transforms state from the limit cycle to the chaotic state. The coexisting chaotic attractors are shown in Fig. 7b. They are evolved from the coexisting limit cycles after many periods. When $d = 2.6$, the system is in the coexisting limit cycles with period-3 as shown in Fig. 7c. With the parameter d varying, this pair of coexisting limit cycles evolved into the coexisting hyperchaotic attractors. The system shows different topological structures with varying d , and we can see that the hyperchaotic memristive system has rich dynamic characteristics.

4.4 Mode of coexisting bifurcation

The coexisting bifurcation mode is essentially a phenomenon of coexisting oscillation. With the varying initial value, different topological structures produced in the same plane of bifurcation diagram. Keeping other parameters the same as mentioned above and select d is the variable parameter. The blue bifurcation diagram generated from the initial state $(1, 1, 1, 1, 0)$, while the red bifurcation diagram generated from the initial state $(-1, -1, -1, -1, 0)$. When the range of parameter d is $[2, 3.5]$, the system has the phenomenon of coexisting bifurcation. As Fig. 8 shown, we can see that the coexisting periodic state and the coexisting chaotic

Fig. 11 Attractors observed in circuit simulation. **a** $x-z$ plane $R_4 = 7.05 \text{ k}\Omega$. **b** $x-z$ plane $R_4 = 8.05 \text{ k}\Omega$. **c** $y-z$ plane $R_4 = 7.05 \text{ k}\Omega$. **d** $y-z$ plane $R_4 = 8.05 \text{ k}\Omega$



state. When the range of parameter d is $[2.82, 2.85]$, we can obtain the coexisting hyperchaotic state. There are many missing parts on their own phase plane, but they complement each other. Finally, a complete bifurcation diagram is formed. The coexisting state reflects the sensitivity and dependency of system to the initial value.

5 Circuit implementation of the system

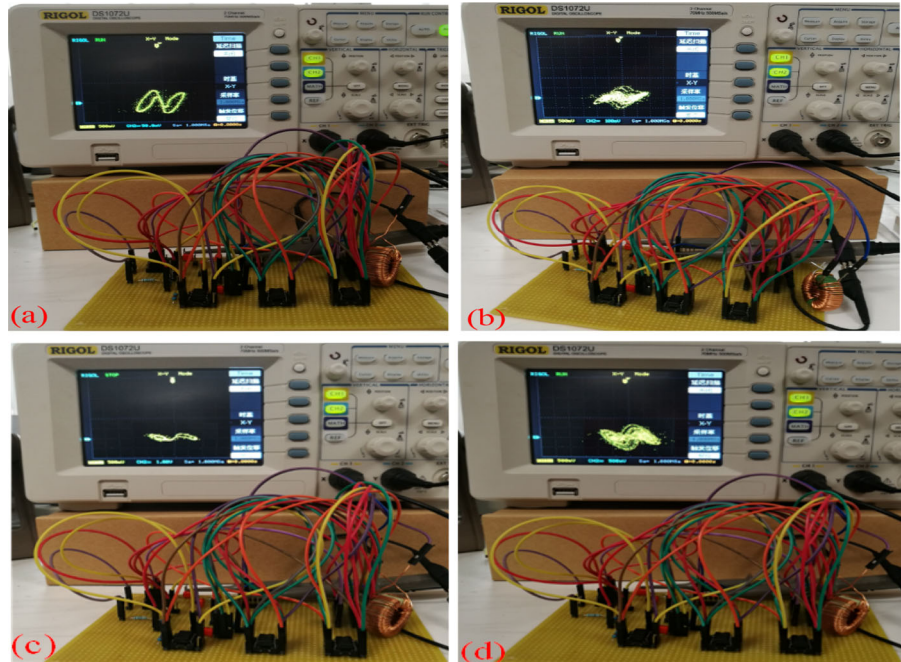
Using NI Multisim 14.0 software of circuit simulation. We use a 3D flux-controlled memristor equivalent circuit to replace the resistance R_1 of the 4D Wien-bridge chaotic circuit. As shown in Fig. 9, we can rebuild a new hyperchaotic memristive circuit. In particular, select the circuit parameters of hyperchaotic memristive circuit $R_1 = 2.0 \text{ k}\Omega$, $R_2 = 5.6 \text{ k}\Omega$, $R_3 = 1 \text{ k}\Omega$, $C_1 = C_2 = C_3 = 33 \text{ nF}$ and $L_1 = 10 \text{ mH}$, the model of the operational amplifier is OP07, and the model of two nonlinear diodes D_1 and D_2 are all 1N4148. Figure 10 shows the equivalent circuit of memristor $R_a = R_b = 10 \text{ k}\Omega$, $R_w = 2 \text{ k}\Omega$, $C_w = 33 \text{ nF}$, the model of the multiplier is AD633, and the model of the operational amplifier is OP07. By adjusting the variable resistor R_4 , the phase diagrams of attractors in different

states can be observed on the oscilloscope. The periodic orbits and the hyperchaotic orbits are shown in Fig. 11. Finally, as shown in Fig. 12, the practical circuit is designed and completed. The experimental results and the conclusions of theoretical analysis are basically the same.

6 Conclusions

A new 5D Wien-bridge hyperchaotic memristive circuit was designed, then the normalized parameter mathematical model was rebuilt. The phenomenon of coexisting attractor was observed, and the mode of coexisting bifurcation was found. The dynamic behaviors of system were analyzed by using the conventional method. With different initial states and varying circuit parameters, the system display rich dynamical characteristics. The circuit simulation was realized by using the equivalent circuit, the parameters of all components have been found. Finally, the practical circuit has been realized successfully. It makes the theoretical analysis and the practical circuit closely together. Therefore, based on these findings and researches, we can obtain the new hyperchaotic memristive circuit system is different from the ordinary chaotic circuit systems.

Fig. 12 Attractors observed in circuit experiment. **a** $x-z$ plane $R_4 = 7.05 \text{ k}\Omega$ **b** $x-z$ plane $R_4 = 8.05 \text{ k}\Omega$ **c** $y-z$ plane $R_4 = 7.05 \text{ k}\Omega$ **d** $y-z$ plane $R_4 = 8.05 \text{ k}\Omega$



The conclusions of theoretical analysis and the results of circuit implementation are basically the same. It shows that the Wien-bridge hyperchaotic circuit system has very rich dynamical behaviors. All these above provide the theoretical guidance and the practical significance for the research of chaotic memristive circuit. In particular, it can be widely used in the field of chaotic encryption and synchronous control. Next, we will try to find more hyperchaotic characteristics in the Wien-bridge hyperchaotic memristive circuit.

Acknowledgements This work supported by the Provincial Natural Science Foundation of Liaoning (Grant No. 20170540060).

References

- Bao, B.C., Liu, Z., Xu, J.P.: New chaotic system and its hyperchaos generation. *J. Syst. Eng. Electron.* **20**, 1179–1187 (2009)
- Bao, B.C., Li, C.B., Xu, J.P., Liu, Z.: New robust chaotic system with exponential quadratic term. *Chin. Phys. B* **17**, 4022 (2008)
- Lü, J.H., Chen, G.R.: A new chaotic attractor coined. *Int. J. Bifurc. Chaos* **12**, 659–661 (2002)
- Bao, B.C., Bao, H., Wang, N., Chen, M., Xu, Q.: Hidden extreme multistability in memristive hyperchaotic system. *Chaos Solitons Fractals* **94**, 102–111 (2017)
- Mou, J., Sun, K.H., Wang, H.H., Ruan, J.Y.: Characteristic analysis of fractional-order 4D hyperchaotic memristive circuit. *Math. Probl. Eng.* **8**, 1–13 (2017)
- Bao, B.C., Xu, Q., Bao, H., Chen, M.: Extreme multistability in a memristive circuit. *Electron. Lett.* **52**, 1008–1010 (2016)
- Bilotta, E.: A gallery of Chua attractors. *Int. J. Bifurc. Chaos* **17**, 49–51 (2015)
- Wang, G.Y., He, J.L., Yuan, F., Peng, C.J.: Dynamical behaviors of a TiO_2 memristor oscillator. *Chin. Phys. Lett.* **30**, 468–477 (2013)
- Ventra, M.D.: Memory effects in complex materials and nanoscale systems. *Adv. Phys.* **60**, 145–227 (2016)
- Tour, J.M., He, T.: Electronics: the fourth element. *Nature* **453**, 42–43 (2008)
- Strukov, D.B., Snider, G.S., Stewart, D.R., Williams, R.S.: The missing memristor found. *Nature* **453**, 80–83 (2008)
- Zeng, D., Zhang, R., Liu, Y., Zhong, S.: Sampled-data synchronization of chaotic Lur'e systems via input-delay-dependent-free-matrix zero equality approach. *Appl. Math. Comput.* **315**, 34–46 (2017)
- Yu, P.: Analysis on double hopf bifurcation using computer algebra with the aid of multiple scales. *Nonlinear Dyn.* **27**, 19–53 (2002)
- Wang, X., Liu, C.: A novel and effective image encryption algorithm based on chaos and DNA encoding. *Multimed. Tools Appl.* **76**, 1–17 (2016)
- Seth, A., Sherman, M., Eastman, P., Delp, S.: Minimal formulation of joint motion for biomechanisms. *Nonlinear Dyn.* **62**, 291–303 (2010)
- Pershin, Y.V., Ventra, M.D.: Experimental demonstration of associative memory with memristive neural networks. *Neural Netw.* **23**, 881–886 (2010)

17. Zeng, D., Zhang, R., Zhong, S., Wang, J., Shi, K.: Sampled-data synchronization control for Markovian delayed complex dynamical networks via a novel convex optimization method. *Neurocomputing* **266**, 606–618 (2017)
18. Shin, S., Kim, K., Kang, S.M.: Memristor applications for programmable analog ICs. *IEEE Trans. Nanotechnol.* **10**, 266–274 (2011)
19. Witrals, K.: Memristor-based stored-reference receiver—the UWB solution. *Electron. Lett.* **45**, 713–714 (2009)
20. Zhang, R., Zeng, D., Zhong, S.: Novel master–slave synchronization criteria of chaotic Lur’e systems with time delays using sampled-data control. *J. Franklin Inst.* **354**, 4930–4954 (2017)
21. Zhang, R., Zeng, D., Zhong, S., Yu, Y.: Event-triggered sampling control for stability and stabilization of memristive neural networks with communication delays. *Appl. Math. Comput.* **310**, 57–74 (2017)
22. Ju, H.P.: Adaptive synchronization of hyperchaotic Chen system with uncertain parameters. *Chaos Solitons Fractals* **26**, 959–964 (2005)
23. Zeng, H.B., Ju, H.P., Xiao, S.P., Liu, Y.J.: Further results on sampled-data control for master-slave synchronization of chaotic Lur’e systems with time delay. *Nonlinear Dyn.* **82**, 1343–1354 (2015)
24. Tae, H.L., Ju, H.P.: Adaptive functional projective lag synchronization of a hyperchaotic Rössler system. *Chin. Phys. Lett.* **26**, 090507 (2009)
25. Zakhidov, A.A., Jung, B., Slinker, J.D., Abruña, H.D., Malliaras, G.G.: A light-emitting memristor. *Org. Electron.* **11**, 150–153 (2010)
26. Wang, X., Chen, Y., Xi, H., Li, H., Dimitrov, D.: Spintronic memristor through spin-torque-induced magnetization motion. *IEEE Electron Device Lett.* **30**, 294–297 (2009)
27. Torrezan, A.C., Strachan, J.P., Medeiros-Ribeiro, G., Williams, R.S.: Sub-nanosecond switching of a tantalum oxide memristor. *Nanotechnology* **22**, 485203 (2011)
28. Kuang, J.L., Leung, A.: Chaotic flexural oscillations of a spinning nanoresonator. *Nonlinear Dyn.* **51**, 9–29 (2008)
29. Sumali, H., Younis, M.I., Abdel-Rahman, E.M.: Special issue on micro- and nano-electromechanical systems. *Nonlinear Dyn.* **54**, 1–2 (2008)
30. Liu, D., Cheng, H., Zhu, X., Wang, G., Wang, N.: Analog memristors based on thickening/thinning of Ag nanofilaments in amorphous manganite thin films. *Appl. Mater. Interfaces* **5**, 11258 (2013)
31. Chua, L.O.: Resistance switching memories are memristors. *Appl. Phys. A* **102**, 765–783 (2011)
32. Chua, L.O.: Memristor—the missing circuit element. *IEEE Trans. Circuit Theory* **18**, 507–519 (1971)
33. Li, Z.J., Zeng, Y.C., Li, Z.B.: Memristive chaotic circuit based on modified SC-CNNs. *Acta Physica Sinica* **63**, 10502–010502 (2014)
34. Bao, B.C., Liu, Z., Xu, J.P.: Dynamical analysis of memristor chaotic oscillator. *Acta Physica Sinica* **59**, 3785–3793 (2010)
35. Bao, B.C., Hu, F.W., Liu, Z., Xu, J.P.: Mapping equivalent approach to analysis and realization of memristor-based dynamical circuit. *Chin. Phys. B* **23**, 303–310 (2014)
36. Vebtra, M.D., Pershin, Y.V., Chua, L.O.: Circuit elements with memory: memristors. *Proc. IEEE Memcapacitors Meminductors* **97**, 1715–1716 (2009)
37. Yang, X.S., Li, Q.: Chaos generator via Wien-bridge oscillator. *Electron. Lett.* **38**, 623–625 (2002)
38. Bao, B.C., Liu, Z., Xu, J.P.: Transient Chaos in smooth memristor oscillator. *Chin. Phys. B* **19**, 158–163 (2010)
39. Bao, B.C., Liu, Z., Xu, J.P.: Steady periodic memristor oscillator with transient chaotic behaviours. *Electron. Lett.* **46**, 237–238 (2010)